ORIGINAL PAPER

Mining-induced mechanical response of coal and rock at different depths: a case study in the Pingdingshan Mining Area

Ersheng Zha[1,2] · Shiyong Wu[3] · Zetian Zhang[1,2] · Ru Zhang[1,2] · Man Wang[4] · Jifang Zhou[3] · Zhaopeng Zhang[2] · Zheqiang Jia[1]

Abstract

To explore the mining-induced mechanical response of coal at different depths, laboratory testing results and field initial geostress data are combined with the geological conditions to study the differences in mining-induced stress and deformation characteristics of the coal and rock at five different depths (300, 600, 700, 850, and 1050 m) by using FLAC^{3D} software. The results show that with increasing mining depth, the abutment pressure increases, and the abutment pressure along the excavation direction at 1050 m is 7 times that at 300 m. With increasing mining depth, the deformation of the roof abscission layer gradually increases, and the deformation along the excavation direction at 1050 m is 4.6 times that at 300 m. The numerical simulation results are consistent with the field monitoring results, meaning that the results are reliable. By further forecasting the mining-induced stress and deformation characteristics of coal and rock deeper than 1000 m (namely, at 1200, 1500, and 1800 m), it is concluded that the abutment pressures at 1200, 1500, and 1800 m are 9, 11, and 14 times that at 300 m, and the roof abscission layer displacements at 1200, 1500, and 1800 m are 6, 8, and 10 times that at 300 m, which coincides with the large deformation trend observed in deep roadways. These results have a certain guiding significance for deep energy exploration and deep coal exploitation.

Keywords Coal and rock · Different depths · Mining-induced mechanical response · In situ stress

Introduction

Worldwide, coal is still in common use, especially in China. In 2018, China's Ministry of Land and Resources released the latest China Mineral Resources Report, showing that coal accounted for 60.4% of the energy consumption structure in 2017, and coal still dominates China's energy consumption structure (Ministry of Natural Resources, PRC 2018). However, because shallow coal resources are gradually being depleted, exploitation of deep coal resources will become inevitable.

An underground coal seam in a rock mass is in an initial stress state before mining. During the mining process, the surrounding rock is deformed on a large scale, resulting in stress redistribution. This redistribution directly affects the stress environment of the coal and rock mass during the mining process and thus affects the mechanical response of the coal and rock mass. Therefore, it is very important to study and quantify the mechanical response of coal and rock masses during mining. Existing research on the mechanical response of coal and rock masses during mining can be divided into two categories: mining-induced abutment pressure distribution and mining-induced displacement evolution.

In the theoretical study of mining-induced abutment pressure, Qian (1981) and Qian and Miao (1995) proposed the idea of combining the "large structure" of overlying strata with the "small structure" of stope support and further proposed the masonry beam theory (Zhang et al. 2003). The structure and equilibrium conditions of the overlying strata

✉ Zetian Zhang
znthe123@126.com

[1] State Key Laboratory of Hydraulics and Mountain River Engineering, Sichuan University, Chengdu 610065, China

[2] MOE Key Laboratory of Deep Underground Science and Engineering, College of Water Resource & Hydropower, Sichuan University, Chengdu 610065, China

[3] Yalong River Hydropower Development Company, LTD, Chengdu 610051, China

[4] State Key Laboratory of Coking Coal Exploitation and Comprehensive Utilization, China Pingmei Shenma Group, Pingdingshan 467000, China

were proposed, laying a foundation for demonstrating the pressure control parameters of the stope. Song (1988) proposed the rock beam transmission hypothesis, divided the formation and development of the abutment pressure into five stages according to the mining pressure theory of the stope, and summarised the expression of abutment pressure distribution under the limit state. Xie et al. (2011) summarised the distribution of abutment pressure at long-wall coal faces during non-pillar mining (NM), top-coal caving mining (TCM), and protective coal seam mining (PCM) through field monitoring data collected in coal mines in Shanxi and Anhui provinces. Based on the theory of existing stope pressure, Kang et al. (2009) selected FLAC^{3D} software to analyse the no. 3 coal seam of the Jincheng Sihe Coal Mine in Shanxi Province and plotted the curves of the change in stress in front of and behind the working face. By analysing the monitoring abutment pressure distribution in the Xinwen Panxi coal mine, it was concluded that the stress concentration factor α of the leading abutment pressure of the mining face was approximately 2.5 (Kang 2013). Wang et al. (2012) used the SIMBURST software to analyse the distribution of abutment pressure in front of a roadway during the step-by-step mining process and obtained the distribution law of mining pressure. Zhao et al. (2011) used the ANSYS software to analyse the abutment pressure concentration coefficient of a coal seam under NM in different mining conditions with different coal column widths and different mining lengths. Yang et al. (2011a, 2011b) used FLAC^{3D} software to calculate the stress distribution in front of a coal mining face under PCM and the stress evolution under the mining conditions. Salmi et al. (2019) has systematically studied the long-term stability of coal pillars and the effect of post-mining subsidence based on rock mass gradual deterioration after mining. And Liu et al. (2020) used FLAC to study the stability and design of roadways in adjacent coal seams.

In the evolution of mining-induced displacement, Wang et al. (1985) used the viscous fluid finite element method to analyse the surrounding rock of a soft rock roadway and showed the influence of the viscous coefficient of the support layer and surrounding rock on the displacement of the roadway. Sun et al. (2019) proposed a new analytical model to calculate the movement of mining-induced strata on the basis of key stratum theory and the mechanical analysis of overburden. And Yang et al. (2020) has systematically studied the deformation and broken characteristics of the overlying strata in longwall coal mining. Based on the displacement of surrounding rock under different support modes in the Panxi Coal Mine -1100 West Roadway at a depth of 1300 m, Fan et al. (2015) summarised the influence of different support methods on deeply buried roadways. Based on the Huafeng Mine -1080 return air alley in the Xinwen mining area, Kang et al. (2015) used the UDEC software to show the damage of different support schemes to the

surrounding rock, and the results were compared with field data reflecting the effectiveness of the simulation test support. Evert (2001) analysed the displacement of a mine roof and the face during the tunnelling process based on the Hoek-Brown strength criterion.

Although the abovementioned research has systematically expounded the mechanical characteristics of coal and rock masses during mining, most of the existing studies have not quantitatively considered the influence of the depth of mining on the mining-induced mechanical response. The geological structure is more complicated in deep mining than in shallow mining, and a deep coal and rock mass will show different mechanical characteristics than a shallow coal and rock mass (He 2004); for example, increased complexity of the surrounding rock stress field (He and Gao 1998), large deformation and volume expansion characteristics (Jiang et al. 2004; Qu and Li 1995), and abrupt changes in mechanical response (Zhou et al. 2015; Pan et al. 2003) have been observed in deep coal and rock masses. The above characteristics indicate that the mining-induced mechanical behaviour of coal and rock will vary considerably with depth. It is necessary to carry out research on the mining-induced mechanical response of coal and rock considering the influence of mining depth.

Therefore, in this paper, the laboratory triaxial compression testing results of coal from different depths in the Pingdingshan Mining Area by considering the in situ stress environment and physical properties of the samples are considered (Zhang et al. 2019a). By considering initial in situ data and the geological conditions of the working surface at different depths in the Pingdingshan Mining Area, the numerical simulation software FLAC^{3D} is used to numerically simulate the mining-induced response of coal seams at five depths, namely 300, 600, 700, 850, and 1050 m, and the distribution of the stress and deformation of the coal mass in front of the mining faces were obtained and compared with the field monitoring geostress and displacement data to verify the rationality of the model calculation. On this basis, a numerical simulation of the mining-induced process of coal and rock masses deeper than 1000 m in the Pingdingshan Mining Area is carried out to predict and analyse the mining-induced mechanical response of deep coal and rock. These results have a certain guiding significance for deep energy exploration and deep coal exploitation.

Numerical model of the mining-induced mechanical response of coal and rock at different depths

Working face conditions at different depths

The five sampling faces (300, 600, 700, 850, and 1050 m deep) in the Pingdingshan Mining Area in Henan Province,

China, are taken as research objects, as shown in Fig. 1 (Zhang et al. 2019b). Referring to the actual conditions of each working face (Liu et al. 2017), the numerical calculation model of the coal and rock mass at different depths is established using the FLAC^{3D} numerical calculation software. To eliminate the interference of other factors on the results as much as possible, the coal seams of the same group (15$^{\#}$ coal seam) are selected for calculation and analysis, and the positions of five different sampling faces are shown in Fig. 2. The sampling working conditions at different depths are as follows, and the geologic section of each working face is given in Fig. 3:

(1) Mining face 17080 in the no. 12 mine (300 m): The design strike of the working face is 1412.5 m long, the slope length is 172.2~185.3 m, and its depth is 306~408 m. The direct roof is grey sandy mudstone with a thickness of 7.9 m, and the main roof is greyish-white medium-grained sandstone with a thickness of 4.1 m. The seam floor is black and dark-grey sandy mudstone with a thickness of 1.02 m.

(2) Mining face 13330 in the no. 8 mine (600 m): The design strike of the working face is 1370 m long, and the length is 1300 m. The north-south slope is 182.5 m wide, and its depth is 533.7~632.2 m. The average coal seam thickness is 3.2 m; the coal seam inclination angle is low, between 10° and 18°, and 11° on average. The direct roof is a thick dark-grey layered sandy mudstone with a thickness of 7.0 m, the main roof is light grey medium- to fine-grained sandstone with a thickness of 13.6 m, and the seam floor is a thin grey sandy mudstone layer containing muscovite with fine-grained sandstone in the middle and a thickness of 5.2 m.

(3) Mining face 14140 in the no. 8 mine (700 m): The east-west strike of the working face can be mined to a length of 897 m, the north-south slope is 168 m wide, and the burial depth is 630–806 m. The thickness of the coal seam is 3.4~3.85 m, with an average thickness of 3.6 m. The coal seam structure includes a thinned area. The dip angle of the coal seam is 17–28°, with an average of 22°, including a gentle westward dip and steep eastward dip. The direct roof is fine-grained sandstone with a thickness of 6.0 m. The main roof is medium- to fine-grained sandstone with muscovite fragments and has a thickness of 7.8 m, and the seam floor is a thin mudstone layer with a thickness of 3.4 m and expands when exposed to water.

(4) Mining face 24080 in the no. 10 mine (850 m): The design strike of the working face is 1579 m long, the length of the cut is 215 m, and its depth is 631~900 m. The dip angle of the coal seam is 10° to 37°, with an average dip of 24°. The direct roof is sandy mudstone and thin sandstone with an average thickness of 14.5 m. The main roof is greyish-white medium-grained sandstone with an average thickness of 14 m. The seam floor is mudstone and sandy mudstone, which gradually thickens from east to west, with an average thickness of 3.9 m.

(5) Mining face 31010 in the no. 12 mine (1050 m): The design strike of the working face is 1027.5 m, the length of the mining face is 931.5 m, the inclined mining length is 218.4 m, and its depth is 1075~1097 m. The thickness of the coal seam is 2.2–3.4 m, with an average of 3.15 m, and the dip angle of the coal seam is 4–7°, with an average of 5°. The main roof of the coal seam is a moderately
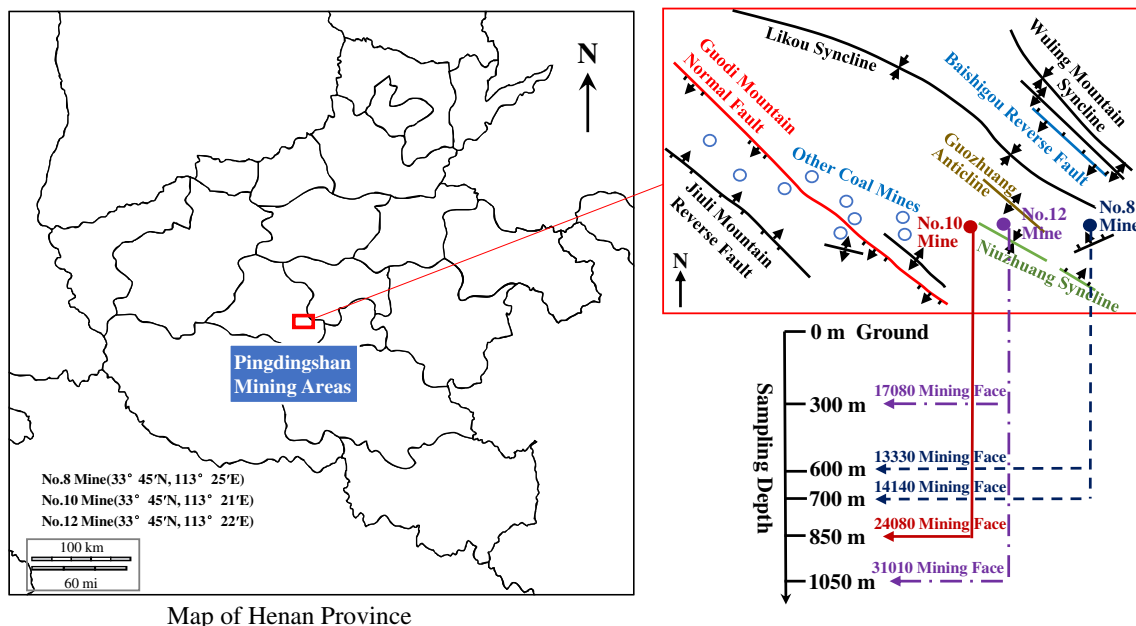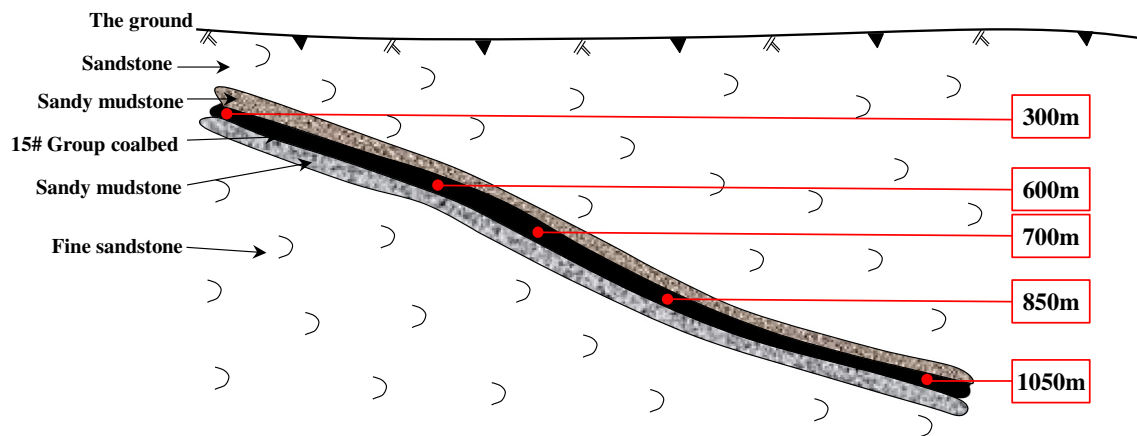

Fig. 1 The location of five sampling faces with different depths in the Pingdingshan Mining Area (Zhang et al. 2019b)

Fig. 2 Diagram of the locations the coal and rock masses at different depths (Zhang et al. 2019a)

thick layer of light-grey to greyish-white medium-grain sandstone with an average thickness of 6 m. The direct roof is greyish-black sandy mudstone. The seam floor is generally dark-grey sandy mudstone or mudstone with a thickness of 0~1.85 m, 0.22 m on average.

Modelling and meshing

According to the geological conditions of the working face, numerical calculation models of coal mining at the different studied depths were established using the FLAC^{3D} numerical simulation software. The dimensions of the model at each depth are 600 m in the x direction, a coordinate range from − 300 to 300 m, and 2 m in the y direction. The height in the z direction varies according to the depth of the model, and the bottom centre of the geologic section (Liu et al. 2017) is taken as the z direction coordinate of 0. To study the evolution of the stress and displacement in front of the working face, a grid of 100 m in front of the face (coordinate range from −50 to 50 m) is refined and five different calculation models are established at different depths. Taking the depth of 1050 m as an example, the constructed model contains 9 rock layers, including the coal seam, whose inclination angle is 5°; the model length is 600 m, the model height is 82.994 m, the model width is 2 m, and a total of 17010 units and 34604 nodes are included, as shown in Fig. 4. And the details of the five models of different depths are shown in Table 1.
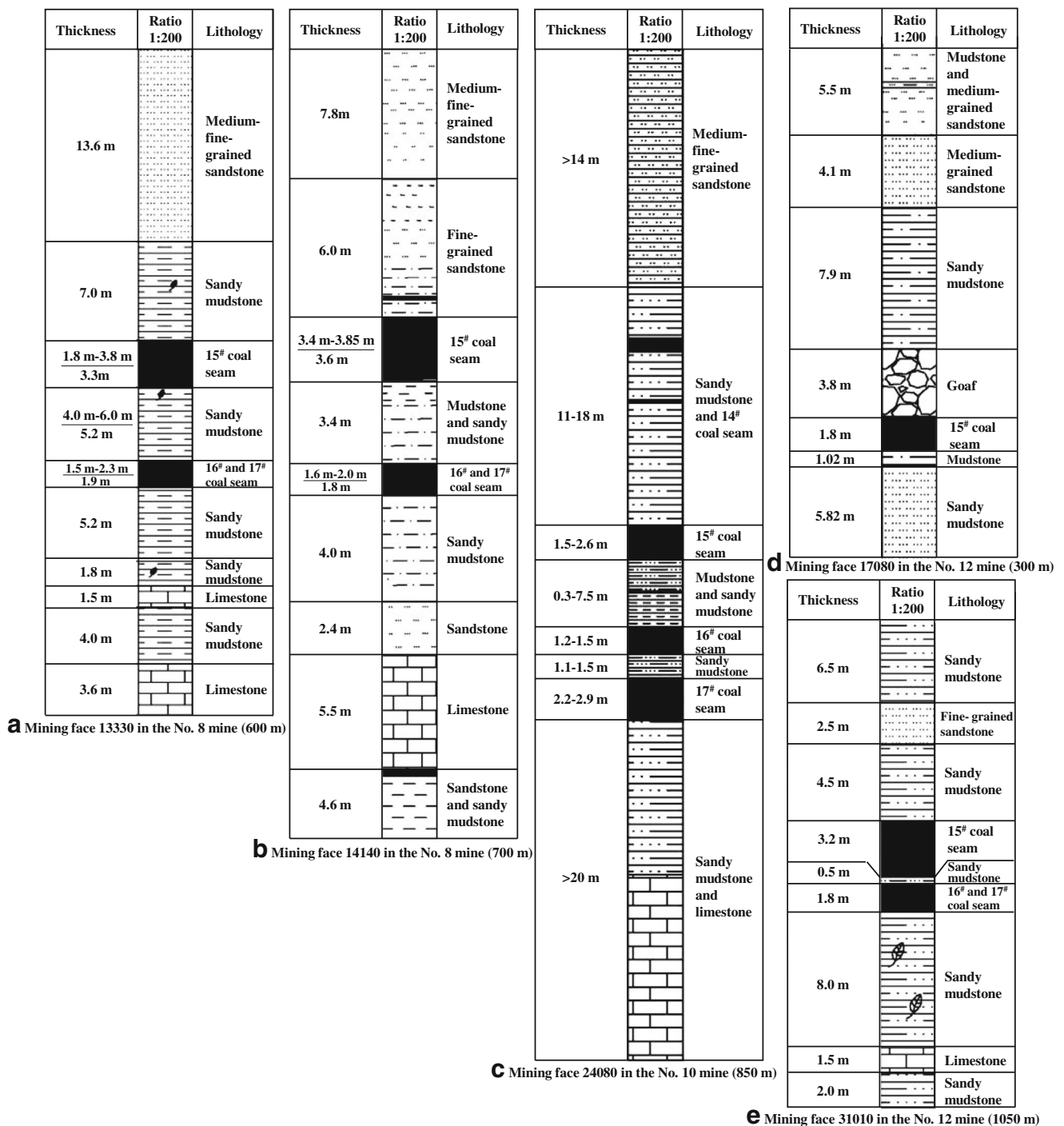
Boundary conditions and load conditions

The boundary conditions and load conditions are determined as follows: (1) A vertical constraint is applied to the bottom of the model to fix the vertical displacement. (2) A horizontal constraint is applied to the left boundary to fix the horizontal displacement. (3) All velocities in the y direction are fixed during calculation. (4) The characteristics of the tectonic stress

in the Pingdingshan Mining Area are obvious, and horizontal stress is the dominant factor. Therefore, the vertical stress (σ_v) is applied at the top boundary according to the initial geostress at different depths, and the maximum horizontal stress (σ_H) is applied to the right boundary according to the initial geostress by applying a gravity gradient to consider the increase in stress with depth. By calculating the in situ stress data of 48 measuring points in the Pingdingshan Mining Area (Zhang et al. 2019a), the lateral pressure ratio coefficient reflecting the relationship between the horizontal ground stress and the vertical ground stress is obtained to consider the horizontal ground stress as a function of depth. The loads applied in the different models are shown in Table 2:

As the coal and rock masses could be assumed as a Mohr-Coulomb material (Sun et al. 2019). And the Mohr-Coulomb failure criterion could reflect the mining-induced mechanical behaviour of coal and rock masses well (Islam et al. 2009; Alehossein and Poulsen 2010), including in the Pingdingshan Mining Area (Gao et al. 2013). Therefore, in our study, the Mohr-Coulomb elastoplastic yield criterion was adopted. The physical and mechanical parameters of the coal in the numerical model were determined by triaxial compression testing of coal and rock considering the physical stress characteristics of the initial stress environment and the depth of the coal (Zhang et al. 2019a), while the physical and mechanical parameters of the rock were determined according to field monitoring data (Gao et al. 2013). The parameters of the coal and rock are shown in Table 3.

Numerical simulation scheme

Considering that the coal seams of each coal mining face in the Pingdingshan Mining Area are not very thick, the coal mining operation is mostly carried out by the NM mining method. Therefore, the whole coal seam section is simulated in the numerical simulation. According to the FLAC^{3D} excavation simulation technology, the vertical displacement and the horizontal displacement are reset after the initial ground stress is applied, and the empty unit is used as the goaf during the excavation

Thickness	Ratio 1:200	Lithology
13.6 m		Medium-fine-grained sandstone
7.0 m		Sandy mudstone
1.8 m-3.8 m / 3.3m		15# coal seam
4.0 m-6.0 m / 5.2 m		Sandy mudstone
1.5 m-2.3 m / 1.9 m		16# and 17# coal seam
5.2 m		Sandy mudstone
1.8 m		Sandy mudstone
1.5 m		Limestone
4.0 m		Sandy mudstone
3.6 m		Limestone

a Mining face 13330 in the No. 8 mine (600 m)

Thickness	Ratio 1:200	Lithology
7.8m		Medium-fine-grained sandstone
6.0 m		Fine-grained sandstone
3.4 m-3.85 m / 3.6 m		15# coal seam
3.4 m		Mudstone and sandy mudstone
1.6 m-2.0 m / 1.8 m		16# and 17# coal seam
4.0 m		Sandy mudstone
2.4 m		Sandstone
5.5 m		Limestone
4.6 m		Sandstone and sandy mudstone

b Mining face 14140 in the No. 8 mine (700 m)

Thickness	Ratio 1:200	Lithology
>14 m		Medium-fine-grained sandstone
11-18 m		Sandy mudstone and 14# coal seam
1.5-2.6 m		15# coal seam
0.3-7.5 m		Mudstone and sandy mudstone
1.2-1.5 m		16# coal seam
1.1-1.5 m		Sandy mudstone
2.2-2.9 m		17# coal seam
>20 m		Sandy mudstone and limestone

c Mining face 24080 in the No. 10 mine (850 m)

Thickness	Ratio 1:200	Lithology
5.5 m		Mudstone and medium-grained sandstone
4.1 m		Medium-grained sandstone
7.9 m		Sandy mudstone
3.8 m		Goaf
1.8 m		15# coal seam
1.02 m		Mudstone
5.82 m		Sandy mudstone

d Mining face 17080 in the No. 12 mine (300 m)

Thickness	Ratio 1:200	Lithology
6.5 m		Sandy mudstone
2.5 m		Fine-grained sandstone
4.5 m		Sandy mudstone
3.2 m		15# coal seam
0.5 m		Sandy mudstone
1.8 m		16# and 17# coal seam
8.0 m		Sandy mudstone
1.5 m		Limestone
2.0 m		Sandy mudstone

e Mining face 31010 in the No. 12 mine (1050 m)

Fig. 3 Geologic section of each working face at the depths studied in this paper (Liu et al. 2017). **a** Mining face 13330 in the no. 8 mine (600 m). **b** Mining face 14140 in the no. 8 mine (700 m). **c** Mining face 24080 in the no. 10 mine (850 m). **d** Mining face 17080 in the no.12 mine (300 m) **e** Mining face 31010 in the no. 12 mine (1050 m)

process. In addition, to reflect the mining-induced evolution process of the stress and displacement of the coal and rock mass in front of the working face, the step-by-step mining method is adopted, and the calculation is carried out once the working face is excavated. The model is considered to converge when the ratio R of the maximum unbalanced force and typical internal force of the system is less than 10^{-4} (Chen 2009). At the same time,

according to the actual mining speed and schedule attained in the field, the initial mining length of the coal seam is 20 m, and then the seam is mined at 4 m per step until a mining length of 60 m is reached. In the coal mining process, the area to 100 m in front of the working face is taken as the main research area, and the quantitative analysis of the stress and displacement distribution in this area is carried out.

Table 1 Details of the calculation models of different depths

Depth (m)	Inclination angle (°)	Height (m)	Number of the strata	Number of the units	Number of the nodes
300	13	164.68	6	13020	26586
600	11	314.22	10	21000	42622
700	22	281.5	9	19110	38824
850	24	326.92	8	13440	27430
1050	5	82.994	9	17010	34604

Mining-induced mechanical response of coal and rock at different depths

Distribution characteristics of abutment pressure

The stress evolution of the coal and rock in front of the working face during the mining process is simulated at different depths. The key monitoring points are placed on the coal seam in front of the mining working face. The key points are
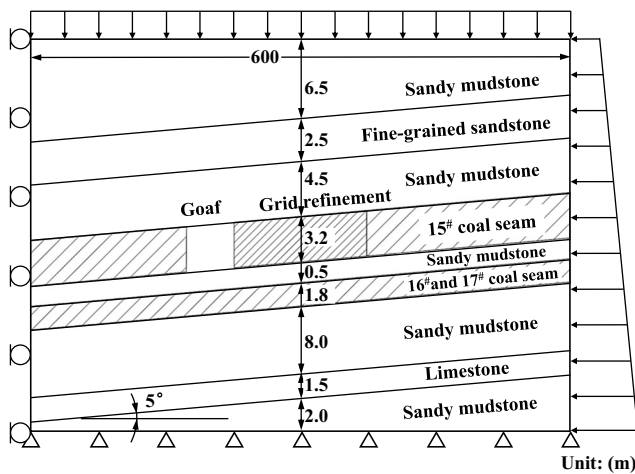
a Diagram of the boundary condition and strata
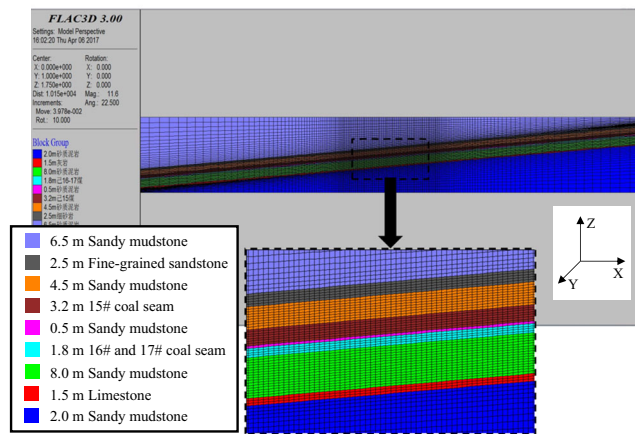
b Modelling and meshing

Fig. 4 Establishment of the numerical model (1050 m model as an example). **a** Diagram of the boundary condition and strata. **b** Modelling and meshing

separated by 1 m, and a total of 100 key points are used to analyse the abutment pressure distribution in front of the working face during the mining process; the abutment pressure distribution curve in front of the working face is obtained at each of the modelled mining depths, as shown in Fig. 5.

The stress distribution curves show that the mining process has destroyed the equilibrium state of the initial rock stress field, causing a redistribution of the stress field of the coal and rock mass. There is an obvious pressure relief area near the working face of the coal seam goaf, and a stress concentration forms in the coal and rock mass in front of the working face. The abutment pressure of the coal seam in the vertical direction shows a certain change with the advancement of the working face. After the stress redistribution, at each of the studied depths, with the advancement of the working face, the abutment pressure of the coal and rock mass in front of working face gradually transits from reflecting the initial stress to the stress concentration and then mining pressure relief (He et al. 2006; Zhang et al. 2006; Hou and Ma 1989).

From the perspective of the overall trend, the abutment pressure distribution curves in front of working faces at different depths are similar: they all increase from the initial stress state. When the peak stress exceeds the strength limit of the coal mass, the abutment pressure in the coal mass gradually decreases to the residual stress, forming a complete space-time evolution, which is consistent with the law of coal mining-induced stress. There are significant differences in the abutment pressure distribution curves in front of working faces for the different mining depths. On the one hand, with increasing depth, the abutment pressures at far from the working face are 5.2, 15.2, 19.1, 21.2, and 25.2 MPa, respectively, and these results are roughly consistent with the field initial

Table 2 In situ stress test results at different depths

Depth (m)	σ_H (MPa)	σ_v (MPa)	σ_h (MPa)
300	14.2	7.6	11.5
600	31.3	17.4	11.0
700	34.4	22.4	20.1
850	40.7	23.5	17.4
1050	43.6	27.2	23.3

Table 3 Parameters of the coal and rock

Rock stratum	Density (kg·m^{-3})	Bulk modulus (GPa)	Shear modulus (GPa)	Friction angle (°)	Cohesion (MPa)	Tensile strength (MPa)
Limestone	2560	6.29	6.92	35	10.2	2.0
Sandy mudstone	2780	11.5	9.5	36	13	6.0
Sandstone	2600	6.5	6.75	38	3.5	3.0
Coal (300 m)	1400	2.67	2.26	30	3	0.28
Coal (600 m)	1400	3.14	2.29	30	3	0.32
Coal (700 m)	1400	3.60	2.56	30	3	0.38
Coal (850 m)	1400	3.63	2.54	30	3	0.49
Coal (1050 m)	1400	3.62	2.50	30	3	0.50

geostress measurements. On the other hand, with an increase in the mining depth, the peak value of the abutment pressure clearly increases from the overall trend; the peak values of the 600, 700, and 850 m models are approximately 4 times that of the 300 m model, while the peak value of the 1050 m model is 7 times that of the 300 m model.

It is found that the abutment pressure peak for 850 m is a little bit lower than that of 700 m in Fig. 5. This is reasonable. In the previous study (Zhang et al. 2019a), the mechanical parameters for the coal samples in the Pingdingshan Mining Area varies nonlinearly with the depth, which is considered in our research in Table 3. In addition, the abutment pressure peak for 850 m is also influenced by geologic section of the working face in Fig. 3 and the in situ stress state in Table 2, resulting the nonlinear increase of the abutment pressure peak among different depths, as well as the position variations of abutment pressure peak among different depths. Note that this stress distribution law is only suitable for this specific situation in the Pingdingshan Mining Area. For different mines and areas, the local geological conditions, coal and rock parameters, and local in situ stress state are suggested to be considered.

Distribution characteristics of the roof abscission layer displacement

The mining of the working face causes not only the stress redistribution of the coal seam but also the large-scale
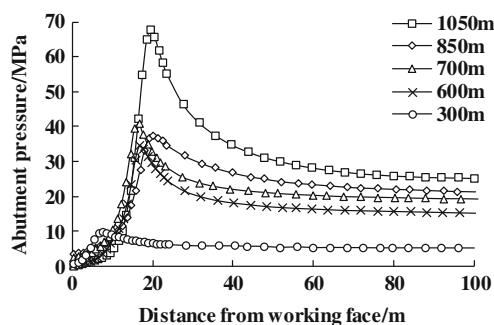
Fig. 5 Abutment pressure distributions at different depths

deformation of the coal and rock mass around the excavation working face. The displacement of the coal and rock mass during the mining process indirectly reflects the stability of the working face. Therefore, numerical simulation of the deformation of the coal and rock mass in front of the mining face at different depths is analysed. In the simulation, the 100 key monitoring points have a spacing of 1 m and obtain the distribution curve of the displacement of the roof abscission layer in front of the working face at different mining depths, as shown in Fig. 6.

Figure 6 shows that the vertical displacement in front of the working face at different depths gradually increases with the advance of the working face and that the distribution can be divided into three areas: The undisturbed area (70–100 m), where the roof abscission layer displacement is small, indicates that the strata are less affected by mining-induced disturbance. The slow growth area (20–70 m) reflects where the roof abscission layer displacement increases gradually but at a slow rate. The rapid growth area (0–20 m) reflects where the roof abscission layer displacement increases sharply; the closer to the working surface, the faster the rate of displacement is. The displacement of the roof abscission layer is maximized at the working face, and the maximum values in the 600, 700, 850, and 1050 m models are 2.8, 3.7, 3.8, and 4.6 times that of the 300 m model, respectively. These results show that the vertical displacement of the roof during the deep mining process is more significant at deeper mining depths and that special attention should be paid to deep mining in the field.

Comparison of numerical simulation results with field monitoring results

The field monitoring experiments have been carried out for coal seams in the Pingdingshan Mining Area in previous studies (Xu 2016; Peng et al. 2018), and the field monitoring data was obtained. Through field in situ monitoring at different depths in the Pingdingshan Mining Area, comprehensive research has been carried out to obtain the mechanical response characteristics of mining-induced rock masses at different depths. In this field monitoring, the distribution curves of the
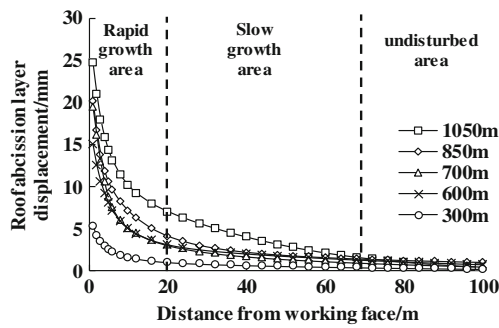
Fig. 6 Roof abscission layer displacements at different depths

abutment pressure in front of the working faces at 850 m and 1050 m and the distribution curves of the displacement of the roof abscission layer at 700, 850, and 1050 m were obtained. The numerical simulation results are compared with the abovementioned field research results to obtain a comparison curve between the numerical simulation and the field monitoring of the abutment pressure, as shown in Fig. 7.

Figure 7 shows that the numerical simulation results of the abutment pressure are consistent with the trend of the field monitoring results. The distributions of the abutment pressure are similar. The distribution of the abutment pressure relief area, the stress concentration area, and the undisturbed stress area in front of the working face is obvious, and these areas are similarly defined by the numerical simulation and field monitoring results. The peak positions of the abutment pressures are close, and all appear within 30 m from the working face. The simulated abutment pressure increasing trend in this area is close to the result of the field study: both show a rapid increase. The influence range of the mining disturbance abutment pressure does not extend far from the working face, and the numerical simulation results and field results suggest this range is approximately 50–70 m.

And there are some differences between numerical simulation results and field test results. The simulation results show that the abutment pressure peak is higher, the distribution curve is smoother, and the abutment pressure at a distance from the working face is closer to the initial geostress, while the field monitoring results show that the abutment pressure peak is lower and that the pressure relief area is larger, which
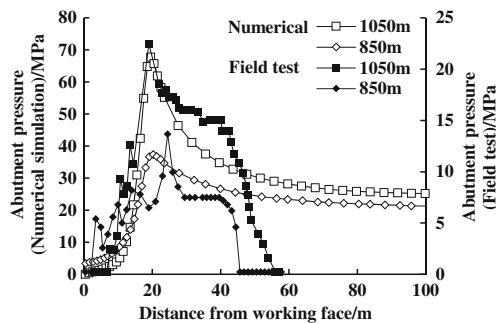
corresponds with the characteristics of the more fractured coal and rock masses observed in actual coal mines. Both results are just the reflection of the mining-induced mechanical behaviour and law, and either testing method may overestimate or underestimate the real stress value, resulting in the differences in abutment pressure values between simulation results and field test results. But it should be noted that the overall trend and distribution law of the simulation results and field test results are similar.

Figure 8 shows a comparison of the numerical simulation and the field monitoring results of the roof abscission layer displacement. The numerical simulation results are consistent with the trend of the field monitoring results. The simulation results show that the changes in the abscission layer displacement at different depths are similar, and both the numerical simulation and the field monitoring results show that the displacement gradually increases from zero displacement in the undisturbed area to the maximum displacement at the working face. The ranges of the undisturbed area, slow growth area, and rapid growth area are approximately the same, and the maximum abscission layer displacement at 1050 m is approximately 25 mm.

The comparison of the numerical simulation results with the field monitoring results shows that the simulation results provide more data, produce more rounded curves, and describe the abutment pressure and the abscission layer displacement distribution and evolution in front of the entire working face for a lower cost. The abutment pressure and the abscission layer displacement distribution curves from the calculation are basically in line with the field monitoring situation, which indicates that the numerical simulation of the mining-induced mechanical response of coal and rock masses at different depths in the Pingdingshan Mining Area is rational and feasible to some extent.

Prediction of the mining-induced mechanical response of coal deeper than 1000 m

On the basis of proving that the coal and rock mass model in the Pingdingshan Mining Area is rational, the changes in the
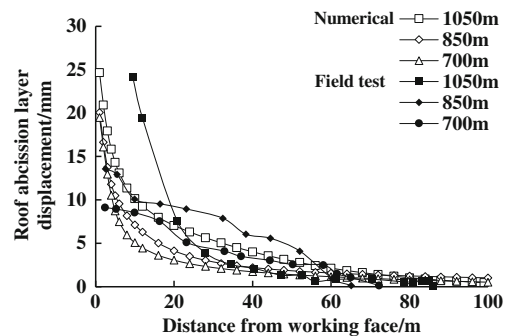

Fig. 7 Comparison of the abutment pressures between numerical simulation results and field monitoring results

Fig. 8 Comparison of roof abscission layer displacements between numerical simulation results and field monitoring results

physical and mechanical parameters of the coal seam and the initial geostress data with depth are fitted to obtain the physical and mechanical parameters and boundary conditions for models deeper than 1000 m. Therefore, numerical models of coal and rock masses at 1200, 1500, and 1800 m depth in the Pingdingshan Mining Area are constructed, and the distribution and evolution of stress and deformation during the mining process of coal from rock masses deeper than 1000 m are analysed by simulating the coal seam mining process. This research has a certain guiding significance for deep coal mining.

Establishment of the coal and rock mass model for coal seams deeper than 1000 m

Because a coal seam deeper than 1050 m in the Pingdingshan Mining Area has not yet been exploited, the working face conditions for deeper mining have not been acquired. Therefore, the geological conditions and the geologic column of the 1050 m working face are selected to represent mining faces deeper than 1000 m (namely, 1200, 1500, and 1800 m), and three deep coal and rock mass models are established. The other parameters used are consistent with the 1050 m calculation model.

The boundary conditions of the model for a coal and rock mass deeper than 1000 m are determined in accordance with the "Boundary conditions and load conditions" section. The load condition is determined by the relationship between the vertical ground stress and the horizontal ground stress with depth (Zhang et al. 2019a) and is obtained by fitting the ground stress data from 48 field measurement points in the Pingdingshan Mining Area. The vertical stress σ_v of the initial geostress is applied to the top boundary of the model deeper than 1000 m, the increase in the geostress with depth is considered by applying a gravity gradient, and the horizontal stress σ_H of the initial geostress is applied to the right boundary. The calculation results of the initial geostress deeper than 1000 m are shown in Table 4.

The Mohr-Coulomb elastoplastic yield criterion is also used in this model. The basic assumptions, calculation methods, and numerical simulation schemes used in the model construction are the same as those described above, and the numerical calculation models of coal seams at 1200, 1500, and 1800 m are obtained.

Distribution and evolution of the abutment pressure and the roof abscission layer displacement of the coal seams deeper than 1000 m

The stress evolution in the coal and rock mass in front of the working face deeper than 100 m during coal mining was simulated, and the distribution curve of the abutment pressure in front of the deep mining face was obtained, as shown in Fig. 9. From

**Table 4** In situ stress calculation for coal seams deeper than 1000 m

Depth (m)	σ_H (MPa)	σ_v (MPa)	σ_h (MPa)
1200	49.2	33.4	23.6
1500	60.6	41.7	27.9
1800	72.0	50.1	32.2

the overall trend of the abutment pressure curves, the evolution of the mining-induced stress environment in front of deep mining faces is consistent. The difference is that the initial values of the deep mining abutment pressures at 1200, 1500, and 1800 m are 31.3, 39.4, and 47.6 MPa, respectively, which are roughly consistent with the vertical initial stress of the coal 1000 m deep in the Pingdingshan Mining Area and gradually increase with mining depth. The stress concentration induced with deeper mining is more significant, and the peak of the abutment pressure clearly increases. The peak abutment pressures at depths of 1200, 1500, and 1800 m are 9, 11, and 14 times, respectively, that at a depth of 300 m. It is noticed that the peak points of the abutment pressure among the three depths get further slowly from the working face with the increase of the depth, and that change is not so obvious. This is because the 1050 m model and coal parameters are still adopted in coal seams deeper than 1050 m. And it is strongly suggested to use the real geological column condition and the coal parameters from the corresponding depth for simulation when the Pingdingshan Mining Area is exploited to the deeper underground in the future.

The evolution of the vertical displacement of the working face during the mining of coal deeper than 1000 m is simulated, as shown in Fig. 10, and the distribution curve of the displacement of the roof abscission layer in front of the mining face is obtained. From the overall trend of the displacement curves, the evolution of the abscission layer displacement in front of mining working faces deeper than 1000 m is consistent and gradually increases with the advancement of the working face, peaking at the working face. The displacements at depths of 1200, 1500, and 1800 m are 6, 8, and 10 times that at a depth of 300 m, respectively, showing that the displacement increase with depth.
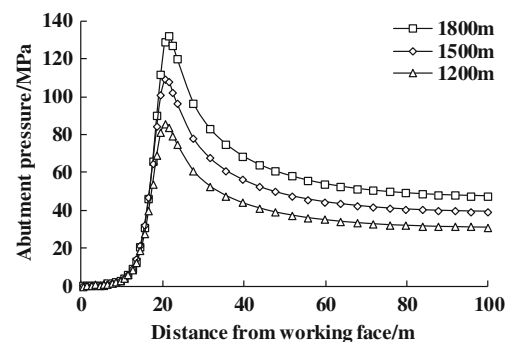
Fig. 9 Abutment pressure distributions in coal seams deeper than 1000 m
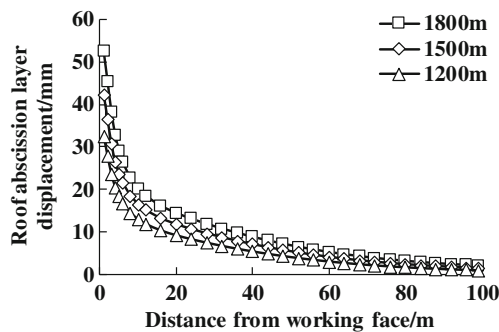
Fig. 10 Comparison of the roof abscission layer displacements in coal seams deeper than 1000 m

In summary, the stress concentration in front of the working face caused by mining is more significant at greater depths below 1000 m, and the abutment pressure of the coal and rock in front of the working face is larger, up to 14 times that at 300 m, corresponding to a stress concentration factor of 2.77; the range of stress redistribution due to mining disturbance is also larger. These phenomena are consistent with the large deformation trend of deep roadways observed in the field.

Conclusions and suggestions

Based on laboratory testing results collected from coal and rock, and initial in situ stress data collected from different depths in the Pingdingshan Mining Area, combined with the actual conditions of working faces at different depths in the Pingdingshan Mining Area, FLAC^{3D} is used to simulate five working faces, and the distributions of the abutment pressure and roof abscission layer displacements of the coal and rock mass in front of a mining face at different depths are obtained; these calculation results are then compared with field monitoring results to verify the rationality of the model calculations. On this basis, the numerical simulation of the mining process of coal deeper than 1000 m is carried to predict and analyse the mining-induced mechanical response of coal and rock masses in the Pingdingshan Mining Area, and the following main conclusions are obtained:

(1) The overall trends in the results suggest that the abutment pressure distributions and evolutions in front of the working faces at different depths are similar. With the increase in mining depth, the values of the initial abutment pressures at depths of 300, 600, 700, 850, and 1050 m are 5.2, 15.2, 19.1, 21.2, and 25.2 MPa, respectively, which are roughly consistent with the field monitoring results. The stress concentration caused by mining disturbance is more significant at greater depths; the abutment pressures at depths of 600, 700, and 850 m are approximately 4 times that at 300 m, while that at 1050 m is 7 times that at 300 m.

(2) The displacement of the roof abscission layer in front of the working face at different mining depths gradually increases with the advancement of the working face and can be divided into undisturbed areas, slow growth areas, and rapid growth areas. The abscission layer displacement is greatest at the working surface, and the maximum values at depths of 600, 700, 850, and 1050 m are 2.8, 3.7, 3.8, and 4.6 times that of 300 m, respectively. The abscission layer displacement of deep mining becomes more significant with depth.

(3) The numerical simulations show the mining-induced distribution and evolution of abutment pressure and abscission layer displacement in front of the working face at different depths are consistent with the trend of the field monitoring results, which indicates that the mining-induced numerical simulation of a coal and rock mass at different depths in the Pingdingshan Mining Area has a certain rationality and feasibility.

(4) Mining below a depth of 1000 m (e.g., at 1200, 1500, and 1800 m) will induce a more significant stress concentration in front of the working face. The abutment pressure of the coal and rock mass in front of the working face during mining is larger below a depth of 100 m, up to 14 times that of 300 m; the corresponding stress concentration factor is 2.77, and the range of mining stress disturbance is also larger. The abscission layer displacement throughout the mining process at 1200, 1500, and 1800 m is 6, 8, and 10 times that at 300 m, respectively, and the abscission layer displacement increases with mining depth. These results are consistent with the large deformation trend of the deep roadways observed in the field, which requires special attention and corresponding engineering precautions.

Nomenclature
Latin symbols R, the ratio of the maximum unbalanced force and typical internal force of the system
Greek symbols σ_h, minimum horizontal stress; σ_H, maximum horizontal stress; σ_v, vertical stress
Abbreviation NM, non-pillar mining; PCM, protective coal seam mining; TCM, top-coal caving mining

References

Alehossein H, Poulsen BA (2010) Stress analysis of longwall top coal caving. Int J Rock Mech Min 47(1):30–41

Chen YM (2009) FLAC/FLAC3D basis and engineering example. China Water & Power Press, Beijing

Evert H (2001) Big tunnels in bad rock. J Geotech Geoenviron 127(9):726–740

Fan MJ, Kang HP, Lin J et al (2015) Study on comprehensive control technology of roadway surroundings with large-dip angle compound strata in coal mine with depth of 1300 m. J Min Safety Eng 32(5):706–713

Gao MZ, Jin WC, Dai ZX et al (2013) Relevance between abutment pressure and fractal dimension of crack network induced by mining. Int J Min Sci Technol 23(6):925–930

He MC (2004) Present situation and prospect of rock mechanics in deep mining engineering. Eighth National Academic Conference on Rock Mechanics and Engineering. Science Press, Beijing, pp 88–94

He MC, Gao EX (1998) Coupled supporting mechanical principle of soft rock roadways and its application. Hydrogeol Eng Geol 2:1–4

He J, He XQ, Nie BS (2006) Monitoring stressed state of coal body by electromagnetic emission. J Min Safety Eng 23(1):111–114

Hou CJ, Ma NJ (1989) Stress in in-seam roadway sides and limit equilibrium zone. J China Coal Soc 1(4):21–29

Islam MR, Hayashi D, Kamruzzaman ABM (2009) Finite element modeling of stress distributions and problems for multi-slice longwall mining in Bangladesh, with special reference to the Barapukuria coal mine. Int J Coal Geol 78(2):91–109

Jiang YD, Zhao YX, Liu WG et al (2004) Research on floor heave of roadway in deep mining. Chin J Rock Mech Eng 23(14):2396–2401

Kang HP (2013) Stress distribution characteristics and strata control technology for roadways in deep coal mines. Coal Sci Technol 41(9):12–17

Kang HP, Wang JH, Gao FQ (2009) Stress distribution characteristics in rock surrounding heading face and its relationship with supporting. J China Coal Soc 34(12):1585–1593

Kang HP, Fan MJ, Gao FQ et al (2015) Deformation and support of rock roadway at depth more than 1000 meters. Chin J Rock Mech Eng 34(11):2227–2241

Liu QY, Zhang R, Wang M et al (2017) Physical properties of coal from different depths. J China Coal Soc 42(8):2102–2110

Liu HT, Qiao BY, Ma NJ (2020) Stability analysis and design of roadways in adjacent seams: a case study from Tashan coal mine in China. Arab J Geosci 13(8):308. https://doi.org/10.1007/s12517-020-05289-8

Ministry of Natural Resources PRC (2018) China mineral resources. Geological Publishing House, Beijing

Pan YS, Li ZH, Zhang MT (2003) Distribution type mechanism and prevention of rockburst in China. Chin J Rock Mech Eng 22(11):1844–1851

Peng Y, Zhang R, Wang M et al (2018) Application of data mining in assessing the roadway stability of mining coal rock at different depths of mines in Pingdingshan. Chin J Rock Mech Eng 37(4):949–960

Qian MG (1981) Conditions required for equilibrium of overlying strata at working areas. J China Univ Min Technol 1(2):34–43

Qian MG, Miao XX (1995) Theoretical analysis on the structural form and stability of overlying strata in longwall mining. Chin J Rock Mechan Eng 14(2):97–106

Qu XX, Li HM (1995) Research on the deformation characteristics of the surrounding rock in soft rock roadways in deep mines. Coal 5:24–26

Salmi EF, Karakus M, Nazem M (2019) Assessing the effects of rock mass gradual deterioration on the long-term stability of abandoned mine workings and the mechanisms of post-mining subsidence-a case study of Castle Fields mine. Tunn Undergr Sp Tech 88:169–185

Song ZQ (1988) Practical method of mine pressure control. China University of Mining and Technology Press, Xuzhou

Sun YJ, Zuo JP, Karakus M et al (2019) Investigation of movement and damage of integral overburden during shallow coal seam mining. Int J Rock Mech Min 117:63–75

Wang R, Liang BY, Sun XY (1985) An analysis of tunnel deformations by the finite element method for viscous fluid. Acta Mech Sinica-PRC 17(2):97–105

Wang G, Cheng WM, Wang HW et al (2012) Numerical simulation research on the distribution of ground stress and pore pressure in front of heading faces. J Shandong Univ Sci Technol (Nat Sci) 31(5):9–14

Xie HP, Zhou HW, Liu JF et al (2011) Mining-induced mechanical behavior in coal seams under different mining layouts. J China Coal Soc 36(7):1067–1074

Xu XL (2016) Research on the stability of mining coal rock mass in different depths in Pingdingshan Mining Area. Sichuan University, Dissertation

Yang W, Lin BQ, Qu YA et al (2011a) Mechanism of strata deformation under protective seam and its application for relieved methane control. Int J Coal Geol 85(3-4):300–306

Yang W, Lin BQ, Qu YA et al (2011b) Stress evolution with time and space during mining of a coal seam. Int J Rock Mech Min 48(7):1145–1152

Yang SL, Song GF, Yang JH (2020) An analytical solution for the geometric broken characteristics of the overlying strata and its physical modeling study in longwall coal mining. Arab J Geosci 13(3):139. https://doi.org/10.1007/s12517-020-5169-3

Zhang XC, Qian MG, Sun BZ (2003) China's Coal Mining Science and Technology. China Coal Industry Publishing House, Beijing

Zhang JG, Lin BQ, Ye Q (2006) Research on technology of draining methane of shallow boreholes in a stress relaxation area of working face. J Min Safety Eng 23(4):432–436

Zhang ZP, Xie HP, Zhang R et al (2019a) Deformation damage and energy evolution characteristics of coal at different depths. Rock Mech Rock Eng 52(5):1491–1503

Zhang ZT, Zhang R, Wu SY et al (2019b) The stress sensitivity and porosity sensitivity of coal permeability at different depths: a case study in the Pingdingshan Mining Area. Rock Mech Rock Eng 52(5):1539–1563

Zhao P, Xie LZ, Xiong L (2011) Numerical simulation of abutment pressure in coal for non-pillar mining. J China Coal Soc 36(12):2029–2034

Zhou H, Meng F, Zhang C et al (2015) Analysis of rockburst mechanisms induced by structural planes in deep tunnels. B Eng Geol Environ 74(4):1435–1451